Available online at www.sciencedirect.com
ScienceDirect
C. R. Physique 10 (2009) 751–763
COMPTES RENDUS PHYSIQUE

Complex and biofluids / Fluides complexes et biologiques

Microconfined flow behavior of red blood cells *in vitro*

Stefano Guido *, Giovanna Tomaiuolo

Dipartimento di Ingegneria chimica, Università di Napoli Federico II, 80125 Napoli, Italy

Available online 17 November 2009

Abstract

The high red blood cell (RBC) deformability is essential to optimal gas exchange between gas and tissues in microcirculation *in vivo*. This review is focused on the flow behavior of RBCs in microconfined geometries *in vitro*, such as circular section capillaries, rectangular channels and pores, where at least one transverse dimension is comparable to cell size. Experimental results on RBC velocity and shape are reviewed together with modeling predictions and numerical simulations. In spite of the progress made so far, the pathophysiological implications of altered RBC deformability are still to be fully elucidated, and more data from clinically-relevant experimental methods and modeling-based interpretation are needed. Future directions include the emerging application of microfluidics techniques to investigate RBC flow in complex geometries. ***To cite this article: S. Guido, G. Tomaiuolo, C. R. Physique 10 (2009).***

Résumé

Comportement des globules rouges dans un écoulement microconfiné *in vitro*. La grande déformabilité des globules rouges (GR) est essentielle pour optimiser les échanges gazeux entre le gaz et la microcirculation dans les tissus *in vivo*. Cette revue est focalisée sur le comportement des GR dans le flux confiné *in vitro*, tels que les capillaires à section circulaire, et les canaux rectangulaire, où au moins une dimension transversale est comparable à la taille des cellules. Résultats expérimentaux sur la vitesse et la forme des GR sont examinés conjointement avec prédictions des modèles et des simulations numériques. En dépit des progrès accomplis à ce jour, les conséquences physiopathologiques des modifications de la déformabilité des GR sont pas encore pleinement élucidées, et autres données expérimentales et de modélisation sont nécessaires. Les directions futures comprennent les nouvelles techniques d'application de la microfluidique pour enquêter sur le flux des GR dans des géométries complexes. ***Pour citer cet article : S. Guido, G. Tomaiuolo, C. R. Physique 10 (2009).***

Keywords: Red blood cell; Deformability; Microcapillary; Microfluidics

Mots-clés : Globules rouges ; Déformabilité ; Capillaries ; Microfluidique

1. Introduction

One of the most striking properties of red blood cells (RBCs) is the high deformability enabling them to flow through microcapillaries with inside diameter even smaller than cell size itself. RBC deformability plays indeed an

* Corresponding author.
E-mail address: steguido@unina.it (S. Guido).

1631-0705/$ – see front matter
doi:10.1016/j.crhy.2009.10.002

essential role in gas transport between blood and tissues [1], mostly occurring in the microcirculation [2], where significant cell deformations both in irregular regions and during cell interactions have been recently observed by *in vivo* high-speed, high resolution imaging [3]. Another example of the physiological relevance of RBC deformability is blood filtration through the spleen vasculature, where older cell clearance is mostly due to trapping in the fenestrated walls of venous sinuses [4]. Here RBCs are forced to squeeze through narrow rectangular slits between endothelial cells having width around 6 μm and height around 1 μm [5,6]. RBC deformability is also an important parameter in evaluating hemocompatibility of artificial devices, such as rotary blood pumps [7], which may induce subhemolytic trauma leading to impaired cell deformability.

In this review, we focus on RBC flow behavior in a microconfined geometry, where at least one dimension is comparable to cell size, such as in microcirculation. Starting from the pioneering work of Fahraeus and Lindqvist [8,9] on the relative apparent viscosity and hematocrit dependence on tube radius, the effects of confinement have been the subject of a number of publications, both from the experimental and modeling side. Literature work on RBC flow in microcapillaries has been reviewed in several papers [10–27]. Recently, RBC confined flow in rectangular microchannels has been also investigated. In fact, the recent progress in the field of microfluidics and lab-on-a-chip devices has attracted much interest in developing blood manipulation and analysis methods at the microscale (see [28] for a review on this promising approach).

This article is organized as follows. In the following section rheological properties of RBCs, which are the major determinants of cell deformability, are described with a short reference to the most used experimental measuring methods. The main fluid dynamic observables related to RBC flow in capillaries, i.e., cell shape and velocity, are the subject of Section 3. Recent results coming from the application of microfluidics techniques are reviewed in Section 4. Concluding remarks and possible future research directions are presented in the last section.

2. Rheological properties of red blood cells

The high deformability allowing RBCs to flow through microcapillaries smaller in size than the cells themselves is attributed to several factors, including cell shape, viscosity of intracellular fluid, and rheological properties of cell membrane [27]. Concerning RBC geometry, the rest shape is a biconcave disk with a major diameter ∼8 μm and thickness ∼2 μm. Such a discoid geometry is in fact an equilibrium configuration between stomatocyte (cup shape) and echinocyte (crenated shape), which is also observed in blood from healthy donors [29,30]. Sodium salicylate (SA)-induced echinocytic shape changes are shown in Fig. 1 [29].

Mean cell volume (MCV) is ∼90 fl and mean surface area (MSA) is ∼135 μm^2, a value significantly greater than the surface area (97 μm^2) of a sphere enclosing a volume of 90 fl [31]. RBC deformability is partly due to this excess area, since under physiological conditions RBC surface area and volume stay constant while flowing in microconfined geometries.

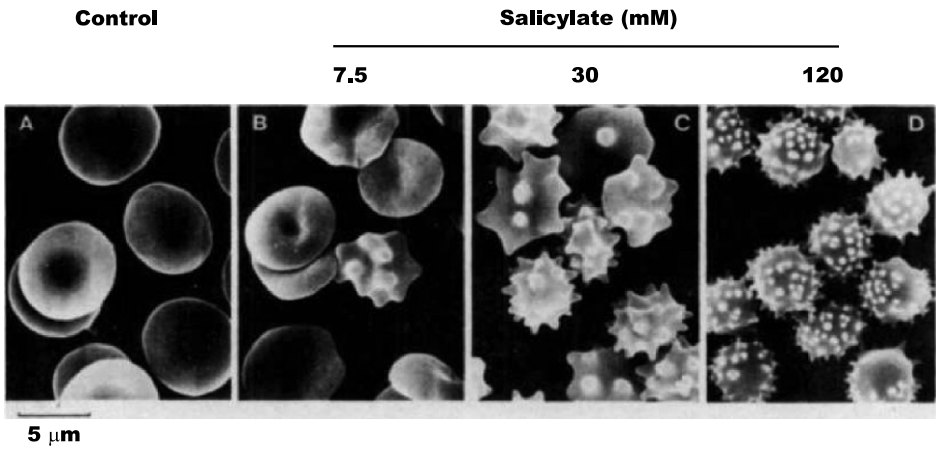

Fig. 1. Scanning electron micrographs of RBCs undergoing sodium salicylate (SA)-induced echinocytic transformation. (A) Normal discocytes. (B) Discocytes and echinocytes at SA = 7.5 mmol/l. (C) Mostly echinocytes at SA = 30 mmol/l. (D) Spheroechinocytes at SA = 120 mmol/l (from [29]).

Table 1
RBC mechanical properties.

	Value	Reference
RBC volume (μm^3)	88.4–107	[31,32,41–50]
Membrane surface area (μm^2)	129.9–141.4	[31,32,41–50]
Membrane surface viscosity ($\mu N\,s/m$)	0.47–1	[51–53]
Cytoplasmic viscosity (mPa s)	6–7	[54,55]
Membrane shear elastic modulus ($\mu N/m$)	1–13	[38,40,52,53,56–61]
Bending elastic modulus ($\times 10^{-19}$ N m)	0.13–3	[62–70]
Time for shape recovery (s)	0.1–0.27	[40,52,71]
Area compressibility modulus (mN/m)	300–500	[36,51,72]

Concerning the intracellular fluid, the rheological behavior is essentially viscous and is dominated by the presence of hemoglobin, whose mean corpuscular concentration (MCHC) is ∼32 g/dl, corresponding to a viscosity of ∼7 mP s [26]. In older cells (RBC life span is about 120 days) both MCV and MSA tend to decrease while maintaining an almost constant ratio [32], and this is associated with an increase of MCHC and inner viscosity [33].

Another key factor affecting RBC deformability is the rheological behavior of the cell membrane, which is a composite material made of a lipid bilayer envelope containing integral proteins, and an underlying protein network referred to as the membrane skeleton [34]. The former is capable of resisting bending (an important property in driving rest shape changes) without having shear resistance, while the latter, which is mainly composed of spectrin, actin, tropomyosin, and proteins 4.1 and 4.9, is responsible for the resistance to stretch and shear deformation [35]. In a two-dimensional continuum mechanics description, the elastic behavior of the RBC membrane is expressed in terms of three fundamental moduli: the shear modulus μ with units of N/m, associated with constant area elongation or shear of the membrane, the area expansion modulus K with units of N/m, corresponding to surface dilation (isotropic expansion) without either shear or bending, and the bending modulus B without either shear or expansion, with units of N m [36].

In a constant area membrane extension, the maximum shear resultant T_s, which is found at 45° to the direction of extension, is related to the extension ratio λ (extended length/original length) by the equation: $T_s = (\mu/2)(\lambda^2 - \lambda^{-2})$. One of the classical methods to measure the shear modulus is micropipette aspiration, which consists of reading the length of the cell portion aspirated into a pipette under a given aspiration pressure [37,38]. As shown in Table 1, the values for μ are in the range 1–10 $\mu N/m$; greater weight was given to values between 6 and 9 $\mu N/m$ due to higher accuracy in measurement of pipette inner diameter [36,39]. A smaller value of 2.5 $\mu N/m$ has been found by RBC elongation through optical tweezers [40]. The difference with respect to the micropipette data was attributed to the large deformations inherent to aspiration in a tiny microcapillary [35].

The micropipette technique has been also used to measure the area expansion modulus K [51]. The simple linear relation between isotropic membrane tension and relative area expansion $T = K \cdot \Delta A/\Delta A_0$ was found, with values of K around 450 mN/m [51]. The assumption of constant surface is indeed based on these high values of the area expansion modulus. More recently, by using fluorescence-imaged micropipette aspiration, the membrane skeleton alone has been probed upon removal of the lipid bilayer, and regions of local dilation and compressibility were observed [73–75].

Finally, the bending modulus B was estimated around 1.8×10^{-19} N m by membrane buckling instability upon micropipette aspiration [62]. Similar values were found by the analysis of thermal fluctuations of the membrane thickness (the flicker phenomenon) [63,76,77], tether formation (see also below) [80], and membrane pulling by atomic force microscopy [65].

RBC rheological behavior is not purely elastic, since membrane fluidity and the intracellular fluid provide a viscous character to the mechanical cell response. This was investigated by the recovery time needed to shape relaxation upon sudden removal of an applied deformation, such as in micropipette aspiration [79]. The recovery time was independent on the initial deformation, and varied from cell to cell in the range 0.1–0.3 s. A measure of membrane viscosity η_m is obtained by multiplying recovery time and shear elasticity modulus. Values around 0.4 $\mu N\,s/m$ were found. Other features related to the viscoelastic behavior of the RBC membrane are formation of thin filaments, referred to as "tethers", induced by yielding of the membrane above a critical stress values [80] (described in terms of a Bingham plastic model), and permanent membrane deformation upon application of a small force for a time scale of a few

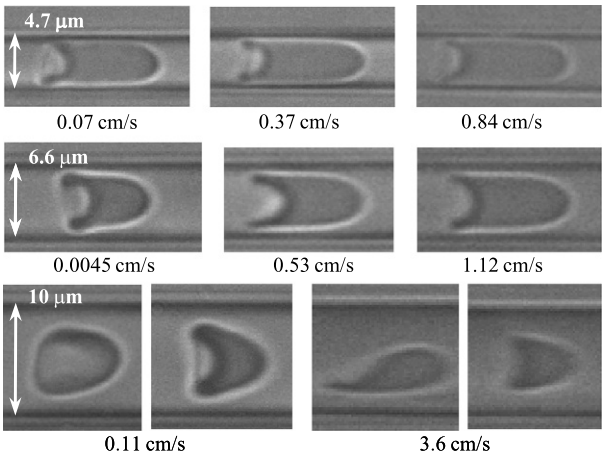

Fig. 2. Images of RBCs flowing *in vitro* in microcapillaries of diameter 4.7, 6.6 and 10 μm at different velocities.

minutes [81]. It should be noticed that according to some authors there is no characteristic relaxation time in creep experiments (the observed trend is a power-law rather than an exponential function) [80,81].

Other techniques to measure RBC deformability include filterability tests [82], pore transit analysis [83,84], laser diffraction ellipsometry (ektacytometry) [85], viscometry [109], rheoscopy [86,87], optical magnetic twisting cytometry [80], defocussing [77] and tomographic phase microscopy [78]. Some of these techniques do not give a direct measure of the viscoelastic constants, but the output is some parameter related to RBC deformability (in some cases of difficult interpretation). A detailed comparison of these techniques, however, is beyond the scope of this review.

3. Red blood cell flow behavior in microcapillaries

Following the classical work of Fahraeus and Lindqvist [8,9] on the relative apparent viscosity and hematocrit dependence on tube radius, RBC confined flow behavior in microcapillaries has been the subject of many investigations. From the experimental side, the main physical observables are cell shape, velocity and thickness of the suspending fluid film separating the cell from the capillary wall, which depend on capillary diameter, pressure drop, and RBC volume fraction in the capillary (commonly referred to as tube hematocrit H_T). In order to adapt to a capillary of inner diameter equal to or smaller than cell size, RBC shape departs from the equilibrium biconcave disk, as observed by *in vivo* experiments [3,110]. The deformed RBC shape *in vivo* has been described as bullet- or parachute-like in some works (e.g., [88], which is based on high-speed imaging of dog mesentery, and in [89–91]). However, in later studies it has been shown that cell deformation at an RBC velocity around 0.1 mm/s is better described in terms of bending or folding around the longitudinal axis, so that the deformed configuration resembles a shallow bowl with a bulging of the forward edge and a thinning of the back end (see [92], which is based on a simultaneous view of RBC motion through two microscopes at right angles). These findings are in contrast with the interpretation of RBC deformation as due to compression and extension in the plane of the original disk by the pressure gradient [93]. More support to nonaxisymmetric RBC shape was provided by microscope examination of cells exposed to a fixative after the passage in a microcapillary at a velocity in the range 0.1–4 mm/s [94].

Recently, RBCs have been imaged at velocities up to ∼5 cm/s in microcapillaries *in vitro* between 10 and 4.7 μm by using a high resolution camera. Samples images are shown in Fig. 2. Asymmetric shapes were mostly observed (together with axisymmetric ones) in the 10 μm microcapillary, as shown in the bottom row of Fig. 2. Up to an RBC velocity around 0.1 cm/s asymmetry was apparently the result of folding of the cell membrane, as found in previous works [93,94]. At higher RBC velocities asymmetric shapes were due to out-of-axis cell position (which is prevented in the smallest microcapillary by the higher confinement) and were indeed associated with a slightly lower cell velocity. Another interesting feature observed in asymmetric cells is membrane rotation (tank-treading), which brings about energy dissipation due to viscous flow of membrane material and cytoplasm [94,96] (whereas cell viscosity does not play a role in the motion of axisymmetrical RBCs). The overall effect of membrane rotation is however to reduce viscous dissipation of the RBC suspension [96], even though the predicted effect on viscosity is small [97]. In the

smallest microcapillary (inside diameter $D = 4.7$ μm) of Fig. 2, RBCs showed an apparently axisymmetric bullet-like shape, possibly due to hemoglobin shifting. The observed trend towards an asymptotic configuration at increasing cell velocity is in agreement with earlier model predictions of Secomb et al. [98], as it will be discussed below.

Another geometric feature associated with RBC shape in confined capillary flow is the geometry of the suspending fluid layer separating the cell body from the confining walls. Indeed, the growth of cell length with velocity is paralleled by a decrease of cell width. Hence, at a given capillary diameter, the layer thickness is an increasing function of cell velocity, with a leveling off at an apparent plateau (∼0.6 μm at a velocity ∼1 mm/s for a capillary diameter of 4.5 μm [99]). At a given velocity, the layer thickness grows with the capillary diameter [99]. The situation is more complex *in vivo* due to the presence of the endothelial glycocalyx, a network of membrane-bound proteoglycans and glycoproteins lining the vascular endothelium with a thickness around 0.5 μm, as reviewed in [100]. Due to the glycocalyx layer, the actual lumen available to plasma and RBC flow is reduced. The glycocalyx is thus considered the main factor leading to the lower flow resistance and the reduced hematocrit found in glass microcapillaries as compared to microvessels *in vivo* [101].

In experiments on capillaries with diameter between 3.3 and 11 μm, RBC velocity v_c was found to consistently exceed the average velocity of the suspending fluid v_p [102]. At any tube hematocrit H_T, the ratio v_c/v_p is a decreasing function of the capillary diameter, going from 1.649 ± 0.128 in the 11 μm capillary to 1.087 ± 0.088 in the 3.3 μm capillary for $H_T = 0.35$. The data, though rather scattered, seem to show an apparent increase of v_c/v_p with cell velocity, a trend supported by recent results [95]. The dependence on capillary diameter is in line with the already mentioned data of the peripheral layer thickness, which decreases more than linearly by lowering capillary diameter [99]. Thus, RBCs occupy a larger fraction of the lumen in capillaries of smaller diameter, and their velocity approaches the average suspending fluid velocity. RBC broadening at low velocities also leads to a decrease in the Fahraeus effect (with the ratio H_T/H_D, where H_D is the discharge hematocrit, closer to unity) [95,102].

The dependence of RBC velocity vs the applied pressure drop has been also investigated. A linear trend has been observed, independently on the viscosity of the suspending fluid [26,95]. RBC velocity has been found relatively unaffected by the hematocrit up to $H_T \sim 20\%$, where trains or *rouleaux* led by a larger cell slightly slowing down the preceding ones have been observed at low pressure gradients (such *rouleaux* disappear at higher pressure drops) [95]. RBC slowing down with increasing cell size has been further confirmed in experiments on dilute suspensions both in capillaries [95] and in microchannels [103]. It can be estimated that the RBC-induced flow disturbance is limited to about one cell length in the single file motion observed in confined capillary flow. Upon increasing the tube hematocrit, bolus motion of intercellular suspending fluid is induced by cell hydrodynamic interactions, as shown in flow visualization experiments [94]. When capillary diameter exceeds 6 μm hematocrit-dependent transition from single- to multi-file (zipper) flow is observed [94].

From the theoretical standpoint, early works, starting from Barnard et al. [104] and Lighthill [105], are based on two key assumptions. In the first place, the RBC, which can be seen as a closely fitting elasto-hydrodynamic pellet, must travel slightly faster than the velocity of the suspension as a whole (as confirmed by the experimental results reviewed above). The resulting leakback takes place in the narrow layer separating the cell surface from the capillary wall and can be modeled by lubrication theory (neglecting inertia). The second assumption is that cell shape is axisymmetric, which is more sound at higher RBC velocity, as pointed out before (see Fig. 2). As a consequence of this assumption, tank-treading does not occur and no viscous contributions to the stress acting on the cell are expected either from the membrane or the intracellular fluid. In the work by Lighthill [105] (which has been extended in [106]), cell deformation is considered proportional to local pressure, which is more suited to describe a solid elastic cell than a fluid-filled sac such as the RBC [94]. In the work by Barnard et al. [104] the stress in the cell membrane is approximated by an isotropic in-plane tension. Secomb et al. [98,107] modeled the membrane by taking into account shear, bending and isotropic tension. The former two are included in the constitutive equation of Evans and Skalak [108], while it is assumed that the cell area remains essentially constant during deformation due to the high value of the elastic modulus of isotropic membrane dilation (around 500 dyn/cm, see Table 1). Thus, for large stresses acting on the membrane at high cell velocity, isotropic membrane tension, which can be generated by small area dilation (as opposed to the large strains which would be induced by shear strains) is dominant in balancing external fluid forces. At lower cell velocities, membrane shear and bending forces become more important, and membrane tension cannot be considered isotropic [98,107]. In the model by Secomb et al., the equations for mechanical equilibrium of an axisymmetric shell are solved together with the lubrication theory equations starting from a spherical unstressed configuration (finite-element calculations starting from a biconcave disk are also provided in [112]).

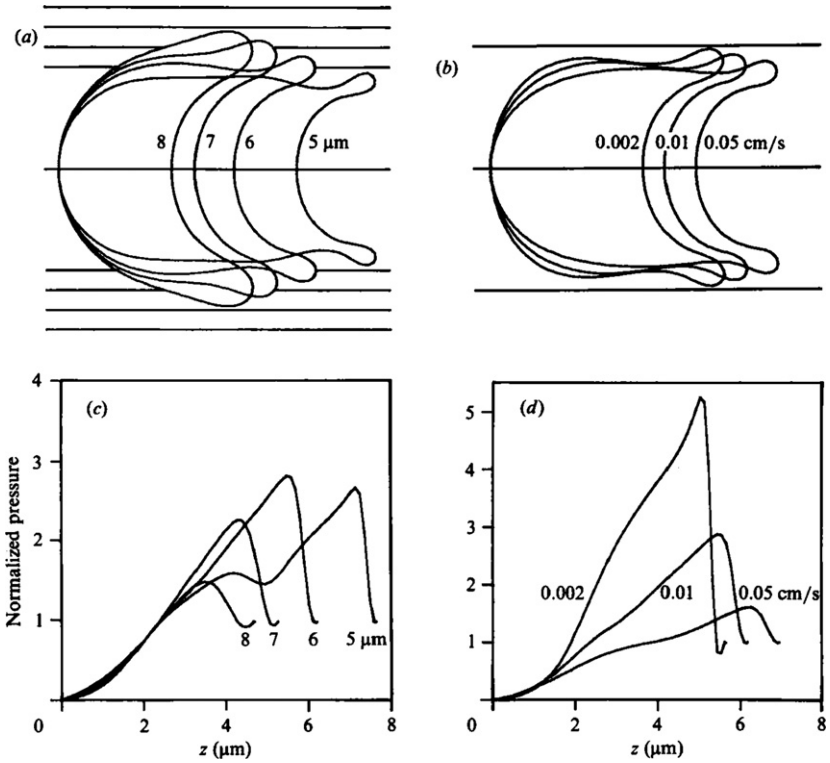

Fig. 3. Predictions of the model by Secomb et al. calculated including both shear and bending elasticity. (a) Cell velocity 0.01 cm/s, vessel diameters as shown. (b) Vessel diameter 6 μm, cell velocities as shown. (c, d) Variation of normalized pressure in the gap corresponding to cell shapes in (a) and (b) (from [98,107]).

Some representative predictions of the model by Secomb et al. [98,107] are shown in Fig. 3, where calculated shapes and the corresponding normalized pressure in the gap are calculated as a function of capillary diameter and cell velocity. The shape results shown in Fig. 3 are in good agreement with the experimental results of Fig. 2 [95]. Further predictions include the viscosity of the cell suspension and the ratio H_T/H_D as a function of cell velocity and capillary diameter. Later extensions of this work were used to model the case of asymmetric cells both in 2D [113] and in 3D [97], and effect of the glycocalyx layer [114,115], as already described. The increase of flow resistance due to nonuniformity of capillary cross-section was also investigated by imposing a sinusoidal diameter variation [54]. It was found that the presence of the glycocalyx layer can mitigate the impact of the increased flow resistance. The effects of membrane viscosity were investigated in analyzing RBC motion through cylindrical micropores, where a significant dependence of transit time on cell size was also found [116].

Axisymmetric motion of a file of RBCs in a capillary has been investigated by Pozrikidis using numerical simulations based on a boundary-integral method for axisymmetric Stokes flow [117–119]. The mathematical formulation adopted by Pozrikidis takes into account the nearly incompressible and elastic properties of the cell membrane with respect to shearing and bending deformation from the unstressed biconcave shape. Since the surface viscosity is not included in the membrane constitutive equation, and the viscosity of the intracellular fluid is assumed to be equal to that of the ambient fluid, the RBC equilibration time is actually underestimated, even though the stationary results are not affected by these simplifying assumptions. An example of the calculated shapes is shown in Fig. 4 at a nondimensional cell separation $L/a = 3$, where L is the distance between cell centers and a is the radius of a sphere having the RBC volume, and at different values of the aspect ratio b/a, where b is the capillary radius, and of the reduced mean velocity $G = \eta v/\mu$, where η is the suspension viscosity, v is the mean suspension velocity and μ the membrane shear modulus. The predicted shapes are in agreement with the axisymmetric experimental ones, as shown in Fig. 2. The results of the numerical simulations are consistent with the predictions of the model by Secomb et al. [98] based on the lubrication approximation.

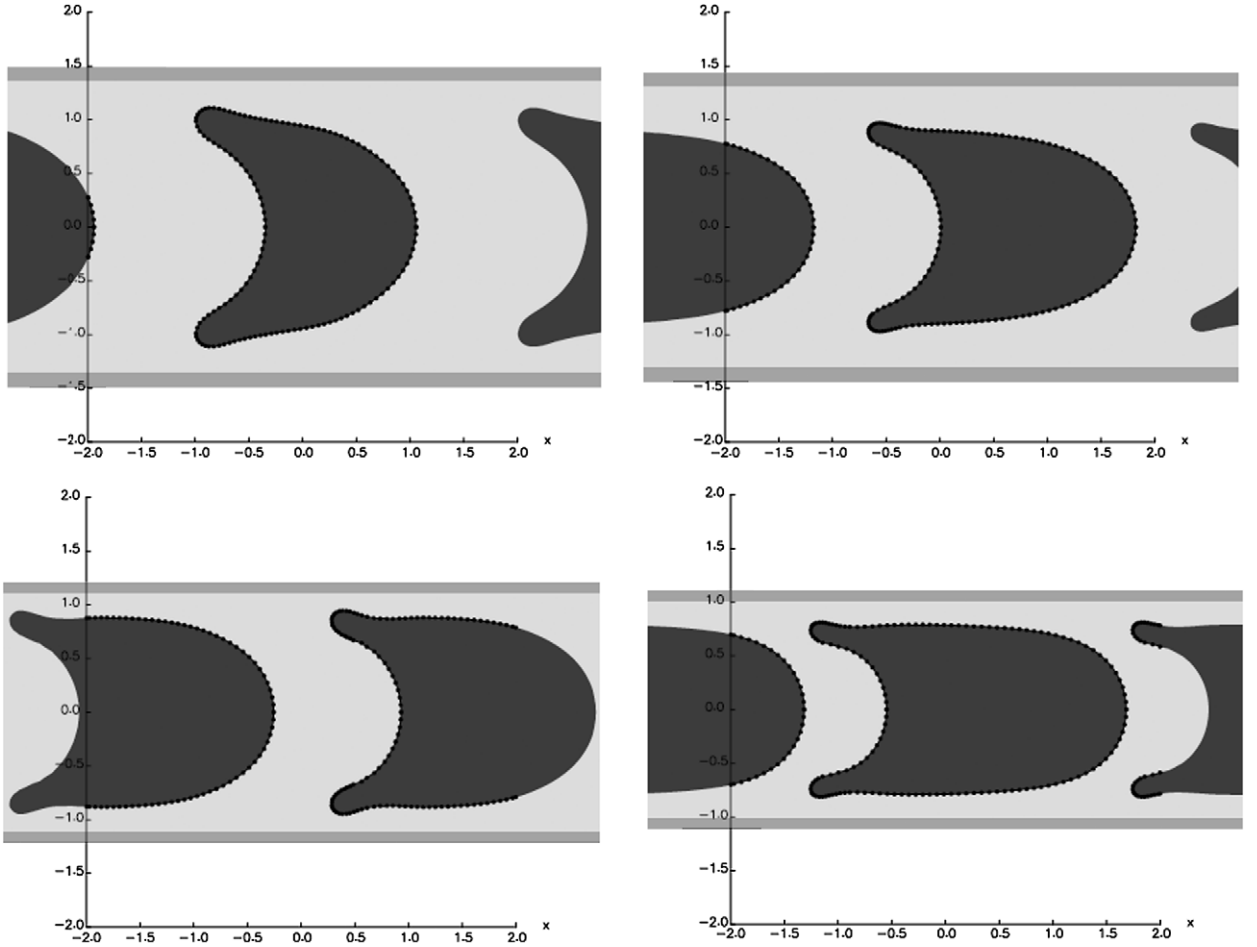

Fig. 4. RBC shapes calculated from numerical simulations by Pozrikidis [118]. The left column corresponds to reduced velocity $G = 0.1$ and $b/a = 1.35$ (top), 1.10 (bottom); the right column corresponds to reduced velocity $G = 0.5$ and $b/a = 1.30$ (top), 1.00 (bottom).

Recently, a coarse-grained numerical approach based on modeling the RBC spectrin network with resolution down to individual junction complexes has been used to analyze large cell deformations [120,121]. Optimal agreement with the already mentioned fluorescence imaging results was found for a pre-stressed RBC configuration [121]. A more complex coarse-grained framework of cytoskeletal dynamics that allows active remodeling of the 3D cytoskeleton via breakable as well as reformable associations of the junction complex and spectrin tetramer has been recently reported [122]. The static equilibrium analysis was extended to the dynamics of RBCs flowing in cylindrical capillaries by using a three-dimensional mesoscopic simulation including a particle-based hydrodynamic model [123]. At a critical velocity increasing linearly with bending rigidity, a model RBC is found to switch from a nonaxisymmetric discocyte to an axisymmetric parachute shape (coaxial with the flow axis). Quite recently, clustering and cell–cell interaction effects in capillary with a radius 1.4 times the equivalent RBC radius have been also studied by the same authors [124]. Following a similar approach, a coarse-grained model was adopted to simulate RBC motion in a microchannel by using dissipative particle dynamics both to describe the cell and the suspending fluid [125]. The results show tank-treading and tumbling motion and the calculated shapes are close to experimental images such as the ones of Fig. 2 [125].

4. RBC flow in microfluidics channels

Microfluidics and miniaturized lab-on-a-chip devices are an emerging new technology with an attractive potential impact for blood analysis [28]. Early work in this area was based on semiconductor processing techniques

and was mainly focused on developing and testing the microdevices, as summarized in the following of this paragraph. Kikuchi et al. reported the fabrication of a filtrometer containing 2600 triangular cross section grooves of typically 6 μm equivalent diameter and 14.4 μm length by means of photolithography and orientation-dependent etching [126,127]. Measurements of the flow rate-pressure curve using straight silicon channels obtained with the same techniques showed non-Newtonian behavior of RBC suspensions [128]. Cylindrical microchannels were also fabricated in glass by an etching method [129]. Silicon micromachining techniques were used to fabricate a microfluidics device incorporating multiple channels of 100 μm length and individual widths ranging between 3.0 and 4.0 μm [130]. By using the so called micromachined haemocytometer it was found that an RBC is a slightly decreasing function of cell size [131], in line with results from glass microcapillaries and microchannels [95,103]. However, a lack of correlation between cell velocity and diameter was found by using a synthetic capillary bed with 2.5- to 4-μm wide channels, possibly due to the combined effect of other concurrent factors [132]. In the same study, cell velocity turned out inversely correlated with intracellular calcium concentration of the cell, which is related to spectrin connectivity and then to cell rigidity [132].

More systematic measurements on RBC deformability were performed by Tsukada et al. [133] by using dry etching straight microchannels in a crystal glass wafer to overcome the limited transparency associated with silicon devices. RBCs flowing in this device at a given pressure head exhibited the classical parachute shape, which was characterized in terms of a deformation index DI given by the ratio of cell length and width. The deformation index was an increasing function of RBC velocity, and DI values of samples from diabetes mellitus patients were found smaller than the ones from healthy donors, thus showing an impaired deformability in the pathological case.

In more recent works, microfluidic devices were fabricated in poly-(dimethylsiloxane) (PDMS), a two-component silicone-based elastomer, by rapid prototyping soft-lithography techniques. Some advantages of this approach are the possibility of mimicking the geometric and structural properties of capillaries, the optical transparency, and the gas permeability. The PDMS soft-lithography technique was applied by Shelby et al. [134] to study the behavior of Plasmodium falciparum-infected RBCs under capillary-like conditions in channels having a depth of 2 μm and width from 2 to 8 μm. While healthy RBCs were able to freely traverse all the channels, malaria infected cells showed an impaired ability (more severe at later stages of infection) to flow through the channels. In the 2-μm channels mechanical expulsion of parasites from RBCs with formation of ghosts was also observed.

Microfluidics techniques have been recently applied to measure dynamical pressure-drop variations along a micrometer-sized channel due to the passage of individual RBCs [26,135]. The measuring method of this differential manometer is based on twin geometry, a test channel where cells flow through, and an identical comparator channel, both of which produce downstream two parallel and adjacent streams of fluid. The liquids flowing through the channels are miscible and the interface downstream is made visible by dyeing the liquid of the comparator channel. The passage of a cell in the test channel brings about a change of the interface position, which can be translated in the cell-induced pressure drop by a calibration procedure. An example of the cell-induced excess pressure drop is shown in Fig. 5. It can be noticed that the experimental trend shows a qualitative agreement with the model predictions of Fig. 3.

Another process which can be studied by the differential manometer is RBC lysis due the blockage of the test section when a cell gets stuck at the channel entrance. This event is followed by an increase of the excess pressure up to a value of 0.4 psi, which is close to that reported in the literature from static micropipette experiments [135] (higher limits, however, can be deduced from channel flow experiments [136]). One advantage of this microfluidics approach is that many cells can be examined in relatively short time, as compared to the micropipette technique.

A well known hydrodynamic effect in microcapillaries is the presence of a cell-free layer adjacent to the wall, which is the basis of the Fahraeus effect [8]. The cross-stream migration leading to the cell-free layer results from hydrodynamic wall repulsion and shear-rate gradients, with the viscosity ratio between the intracellular and outer fluid as a key parameter [137]. By using a microfluidics model, it was found that a geometrical constriction can enhance the size of the cell-free layer [138]. Such geometrical focusing can be applied for RBCs separation from the suspending plasma.

Further developments of the microfluidics approach include the fabrication of complex flow patterns with dimensions and topology similar to microcirculation *in vivo* [139]. By studying the perfusion of a network of channels of different size the effect of glutaraldehyde-induced impairment of RBC deformability has been studied [140]. A higher sensitivity to small deformability changes was found as compared to conventional filterability tests.

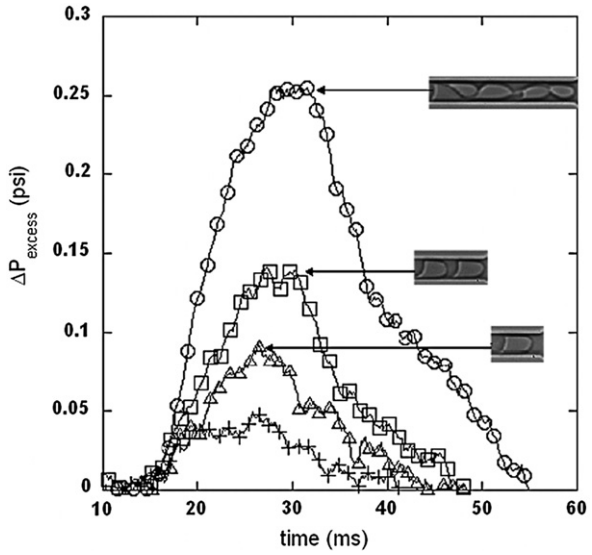

Fig. 5. Pressure drop associated with cell passage vs time. Starting from bottom, the + symbols refer to a healthy RBC, while the open points correspond to RBCs treated with 0.001% glutaraldehyde: one RBC, triangles; a train of two RBCs, squares; a train of five RBCs, circles (mean flow velocity ≈1 cm/s) [135].

5. Conclusions

In this article, flow behavior of RBCs in microconfined geometries has been reviewed. Thus, the focus is on capillaries or channels with one dimension comparable to cell size, where single file motion is mostly observed. Aggregation effects are not taken into account, apart from *rouleaux* formation at increasing hematocrit. Confined RBC flow is a quite active area of research both from the modeling and experimental side, and several significant contributions from the literature have not been included here due to space limitations. For example, significant insight in RBC flow behavior in confined geometries can be gained from model systems, such as deformable bags [111,145, 148], vesicles [137,146,150], capsules [144,147,149] and droplets [151].

One reason of the interest in this subject stems from the possible pathophysiological implications of the viscoelastic RBC properties, which are referred to as cell deformability, since such properties allow a cell to flow in vessels smaller than its own size in the microcirculation. The role of impaired RBC deformability has been investigated in several pathologies, such as sickle cell disease, diabetes, thalassemia, polycythemia, and hereditary elliptocytosis (see [141] for a review). In addition, the effects of drugs on RBC deformability has been studied both *per se* and for the possible role of RBCs as a carrier system for transport and delivery of pharmacological substances [30]. Advanced biophysical methods are now available to probe subcellular components (e.g., Raman microscopy [142]) and can be combined with molecular biology tools to gain a deeper insight on RBC deformability at the molecular level.

While sophisticated methods are now available at a single cell level, more work is needed to develop high-throughput techniques allowing one to get clinically-relevant data from a cell population. A promising approach in this respect is the application of microfluidics devices, which would be in principle capable to separate the blood cellular components too. More experimental and modeling work is needed to fully exploit the potential of microfluidics technology. This includes coupling of classical fluid dynamics with constitutive equations of the RBC rheological response in complex flow geometries. Further studies on the interactions between RBCs and between RBCs and endothelium are also needed [143].

Acknowledgements

Valuable help from Tiziana Mastantuono in looking for most of the papers cited in this work is gratefully acknowledged. The authors acknowledge funding from the Italian Ministry of Research under PRIN 2006 program and from

the Regione Campania under L.R. N.5 of 28/03/2002 (2005 program). Support through the BIOMICS – Biomimetic and Cellular Systems ESA topical team was also helpful for stimulating discussions and meeting opportunities.

References

[1] C.H. Wang, A.S. Popel, Effect of red blood cell shape on oxygen transport in capillaries, Math. Biosci. 116 (1993) 89–110.
[2] P.C. Johnson, Overview of the microcirculation, in: Microcirculation, Academic Press, 2008.
[3] V.P. Zharov, E.I. Galanzha, Y. Menyaev, V.V. Tuchin, In vivo high-speed imaging of individual cells in fast blood flow, J. Biomed. Opt. 11 (2006) 054034.
[4] L.T. Chen, L. Weiss, The role of the sinus wall in the passage of erythrocytes through the spleen, Blood 41 (1973) 529–537.
[5] G.R. Cokelet, Dynamics of erythrocyte motion in filtration tests and in vivo flow, Scand. J. Clin. Lab. Invest. Suppl. 156 (1981) 77–82.
[6] R.A. Freitas Jr., Nanomedicine, Volume IIA: Biocompatibility, Landes Bioscience, Georgetown, TX, 2003.
[7] N. Watanabe, D. Sakota, K. Ohuchi, S. Takatani, Deformability of red blood cells and its relation to blood trauma in rotary blood pumps, Artif. Organs. 31 (2007) 352–358.
[8] R. Fahraeus, The suspension stability of the blood, Physiol. Rev. 9 (1929) 241–274.
[9] R. Fahraeus, T. Lindqvist, The viscosity of the blood in narrow capillary tubes, Am. J. Physiol. 96 (1931) 562–568.
[10] P. Gaethgens, Flow of blood through narrow capillaries. Rheological mechanisms determining capillary hematocrit and apparent viscosity, Biorheology 17 (1980) 183–189.
[11] S. Chien, S. Usami, R. Skalak, Blood flow in small tubes, in: Handbook of Physiology: The Cardiovascular System IV, American Physiological Society, Bethesda, MD, 1984.
[12] B.W. Zweifach, H.H. Lipowsky, Pressure–flow relations in blood and lymph microcirculation, in: Handbook of Physiology: The Cardiovascular System IV, American Physiological Society, Bethesda, MD, 1984.
[13] H.H. Lipowsky, Mechanics of blood flow in the microcirculation, in: Handbook of Biomechanics, McGraw–Hill, Englewood Cliffs, 1986.
[14] T.W. Secomb, Red blood cell mechanics and capillary blood rheology, Cell Biophys. 18 (1991) 231–251.
[15] T.W. Secomb, Mechanics of blood flow in the microcirculation, in: Biological Fluid Dynamics, Company of Biologists, London, 1995, pp. 305–321.
[16] T.W. Secomb, Mechanics of red blood cells and blood flow in narrow tubes, in: Modeling and Simulation of Capsules and Biological Cells, Chapman & Hall, London, 2003.
[17] A.R. Pries, T.W. Secomb, P. Gaehtgens, Biophysical aspects of blood flow in the microvasculature, Cardiovasc. Res. 32 (1996) 654–667.
[18] G. Mchedlishvili, N. Maeda, Blood flow structure related to red cell flow: A determinant of blood fluidity in narrow microvessels, Jpn. J. Physiol. 51 (2001) 19–30.
[19] G.W. Schmid-Schönbein, Biomechanics of microcirculatory blood perfusion, Annu. Rev. Biomech. 1 (1999) 73–102.
[20] R.D. Kamm, Cellular fluid mechanics, Annu. Rev. Fluid Mech. 34 (2002) 211–232.
[21] M. Sugihara-Sekia, B.M. Fu, Blood flow and permeability in microvessels, Fluid Dyn. Res. 37 (2005) 82–132.
[22] V. Cristini, G.S. Kassab, Computer modeling of red blood cell rheology in the microcirculation: A brief overview, Ann. Biomed. Eng. 33 (2005) 1724–1727.
[23] B. M Cooke, C.T. Lim, Mechanical and adhesive properties of healthy and diseased red blood cells, in: Microcirculation, Academic Press, 2008.
[24] H.H. Lipowsky, Microvascular rheology and hemodynamics, Microcirculation 12 (2005) 5–15.
[25] G. Barshtein, R. Ben-Ami, S. Yedgar, Role of red blood cell flow behavior in hemodynamics and hemostasis, Expert Rev. Cardiovasc. Ther. 5 (2007) 743–752.
[26] M. Abkarian, M. Faivre, R. Horton, K. Smistrup, C.A. Best-Popescu, H.A. Stone, Cellular-scale hydrodynamics, Biomed. Mater. 3 (2008) 034011.
[27] S. Chien, Red cell deformability and its relevance to blood flow, Annu. Rev. Physiol. 49 (1987) 177–192.
[28] M. Toner, D. Irimia, Blood-on-a-chip, Annu. Rev. Biomed. Eng. 7 (2005) 77–103.
[29] W.H. Reinhart, S. Chien, Red cell rheology in stomatocyte–echinocyte transformation: Roles of cell geometry and cell shape, Blood 67 (1986) 1110–1118.
[30] H. Dumez, W.H. Reinhart, G. Guetens, E.A. de Bruijn, Human red blood cells: Rheological aspects, uptake, and release of cytotoxic drugs, Crit. Rev. Clin. Lab. Sci. 41 (2004) 159–188.
[31] P.B. Canham, A.C. Burton, Distribution of size and shape in populations of normal human red cells, Circ. Res. 22 (1968) 405–422.
[32] R.E. Waugh, M. Narla, C.W. Jackson, T.J. Mueller, T. Suzuki, G.L. Dale, Rheologic properties of senescent erythrocytes: Loss of surface area and volume with red blood cell age, Blood 79 (1992) 1351–1358.
[33] O. Linderkamp, H.J. Meiselman, Geometric, osmotic, and membrane mechanical properties of density-separated human red cells, Blood 59 (1982) 1121–1127.
[34] J.A. Chasis, S.B. Shohet, Red cell biochemical anatomy and membrane properties, Annu. Rev. Physiol. 49 (1987) 237–248.
[35] H.K. Gerald Lim, M. Wortis, R. Mukhopadhyay, Red blood cell shapes and shape transformations: Newtonian mechanics of a composite membrane, Soft Matter 4 (2008) 83.
[36] R.M. Hochmuth, R.E. Waugh, Erythrocyte membrane elasticity and viscosity, Annu. Rev. Physiol. 49 (1987) 209–219.
[37] S. Chien, K.-L.P. Sung, R. Skalak, S. Usami, Theoretical and experimental studies on viscoelastic properties of erythrocyte membrane, Biophys. J. 24 (1978) 463–487.
[38] E.A. Evans, New membrane concept applied to the analysis of fluid shear- and micropipette-deformed red blood cells, Biophys. J. 13 (1973) 941–954.

[39] E. Evans, N. Mohandas, A. Leung, Static and dynamic rigidities of normal and sickle erythrocytes. Major influence of cell hemoglobin concentration, J. Clin. Invest. 73 (1984) 477–488.
[40] S. Hénon, G. Lenormand, A. Richert, F. Gallet, A new determination of the shear modulus of the human erythrocyte membrane using optical tweezers, Biophys. J. 76 (1999) 1145–1151.
[41] E.A. Evans, Y.C. Fung, Improved measurements of the erythrocyte geometry, Microvasc. Res. 4 (1972) 335–347.
[42] A.W.L. Jay, Geometry of the human erythrocyte. I. Effect of albumin on cell geometry, Biophys. J. 15 (1975) 205–222.
[43] Y.C. Fung, Biomechanics, Springer, New York, 1981.
[44] O.L. Linderkamp, H.J. Meiselman, Geometric, osmotic, and membrane mechanical properties of density-separated human red cells, Blood 59 (1982) 1121–1127.
[45] G.B. Nash, H.J. Meiselman, Red cell and ghost viscoelasticity. Effects of hemoglobin concentration and in vivo aging, Biophys. J. 43 (1983) 63–73.
[46] O.L. Linderkamp, P.Y. Wu, H.J. Meiselman, Geometry of neonatal and adult red blood cells, Pediatr. Res. 17 (1983) 250–253.
[47] O.L. Linderkamp, E. Friederichs, H.J. Meiselman, Mechanical and geometrical properties of density-separated neonatal and adult erythrocytes, Pediatr. Res. 34 (1993) 688–693.
[48] A. Stadler, O. Linderkamp, Flow behavior of neonatal and adult erythrocytes in narrow capillaries, Microvasc. Res. 37 (1989) 267–279.
[49] K.G. Engstrom, E. Lofvenberg, Treatment of myeloproliferative disorders with hydroxyurea: Effects on red blood cell geometry and deformability, Blood 91 (1998) 3986–3991.
[50] P. Ruef, O. Linderkamp, Deformability and geometry of neonatal erythrocytes with irregular shapes, Pediatr. Res. 45 (1999) 114–119.
[51] E.A. Evans, R. Waugh, L. Melnik, Elastic area compressibility modulus of red cell membrane, Biophys. J. 16 (1976) 585–595.
[52] E.A. Evans, R.M. Hochmuth, Membrane viscoelasticity, Biophys. J. 16 (1976) 1–11.
[53] G. Bazzoni, M. Rasia, Effects of an amphipathic drug on the rheological properties of the cell membrane, Blood Cells, Molecules, and Diseases 24 (1998) 552–559.
[54] T.W. Secomb, R. Hsu, A.R. Pries, Blood flow and red blood cell deformation in nonuniform capillaries: Effects of the endothelial surface layer, Microcirculation 9 (2002) 189–196.
[55] Y. Haik, V. Pai, C.-J. Chen, Apparent viscosity of human blood in a high static magnetic field, J. Magn. Magn. Mater. 225 (2001) 180–186.
[56] J. Guck, R. Ananthakrishnan, H. Mahmood, T.J. Moon, C.C. Cunningham, J. Kas, The optical stretcher: A novel laser tool to micromanipulate cells, Biophys. J. 81 (2001) 767–784.
[57] J.C.M. Lee, D.E. Discher, Deformation-enhanced fluctuations in the red cell skeleton with theoretical relations to elasticity, connectivity, and spectrin unfolding, Biophys. J. 81 (2001) 3178–3192.
[58] G. Lenormand, S. Hénon, A. Richert, J. Siméon, F. Gallet, Direct measurement of the area expansion and shear moduli of the human red blood cell membrane skeleton, Biophys. J. 81 (2001) 43–56.
[59] G. Lenormand, S. Hénon, A. Richert, J. Siméon, F. Gallet, Elasticity of the human red blood cell skeleton, Biorheology 40 (2003) 247–251.
[60] R.M. Hochmuth, N. Mohandas, Uniaxial loading of the red cell membrane, J. Biomech. 5 (1972) 501–509.
[61] R. Skalak, A. Tozeren, R.P. Zarda, S. Chien, Strain energy function of red blood cell membranes, Biophys. J. 13 (1973) 245–264.
[62] E.A. Evans, Bending elastic modulus of red blood cell membrane derived from buckling instability in micropipet aspiration tests, Biophys. J. 43 (1983) 27–30.
[63] H. Strey, M. Peterson, E. Sackmann, Measurement of erythrocyte membrane elasticity by flicker eigenmode decomposition, Biophys. J. 69 (1995) 478–488.
[64] W.C. Hwang, R.E. Waugh, Energy of dissociation of lipid bilayer from the membrane skeleton of red blood cells, Biophys. J. 72 (1997) 2669–2678.
[65] L. Scheffer, A. Bitler, E. Ben-Jacob, R. Korenstein, Atomic force pulling: Probing the local elasticity of the cell membrane, Eur. Biophys. J. 30 (2001) 83–90.
[66] A. Zilker, H. Engelhardt, E. Sackmann, Dynamic reflection interference contrast (RIC) microscopy: A new method to study surface excitations of cells and to measure membrane bending elastic moduli, J. Phys. Fr. 48 (1987) 2139–2151.
[67] K. Zeman, H. Engelhard, E. Sackmann, Bending undulations and elasticity of the erythrocyte membrane: Effects of cell shape and membrane organization, Eur. Biophys. J. 18 (1990) 203–219.
[68] M.A. Peterson, Linear response of the human erythrocyte to mechanical stress, Phys. Rev. A 45 (1992) 4116–4131.
[69] A. Humpert, M. Baumann, Local membrane curvature affects spontaneous membrane fluctuation characteristics, Mol. Membr. Biol. 20 (2003) 155–162.
[70] R. Waugh, R. Bauserman, Physical measurements of bilayerskeletal separation forces, Ann. Biomed. Eng. 23 (1995) 308–321.
[71] P.J.H. Bronkhorst, G.J. Streekstra, J. Grimbergen, E.J. Nijhof, J.J. Sixma, G.J. Brakenhoff, A new method to study shape recovery of red blood cells using multiple optical trapping, Biophys. J. 69 (1995) 1666–1673.
[72] R. Waugh, E.A. Evans, Thermoelasticity of red blood cell membrane, Biophys. J. 26 (1979) 115–131.
[73] D.E. Discher, N. Mohandas, E.A. Evans, Molecular maps of red cell deformation: Hidden elasticity and in situ connectivity, Science, New Series 266 (1994) 1032–1035.
[74] D.E. Discher, N. Mohandas, Kinematics of red cell aspiration by fluorescence-imaged microdeformation, Biophys. J. 71 (1996) 1680–1694.
[75] J.C. Lee, D.T. Wong, D.E. Discher, Direct measures of large, anisotropic strains in deformation of the erythrocyte cytoskeleton, Biophys. J. 77 (1999) 853–864.
[76] F. Brochard, J.F. Lennon, Frequency spectrum of the flicker phenomenon in erythrocytes, J. Phys. Fr. 36 (1975) 1035–1047.
[77] L.G. Mesquita, U. Agero, O.N. Mesquita, Defocusing microscopy: An approach for red blood cell optics, Appl. Phys. Lett. 88 (2006) 133901.
[78] Y.K. Park, M. Diez-Silva, G. Popescu, G. Lykotrafitis, W. Choi, M.S. Feld, S. Suresh, Refractive index maps and membrane dynamics of human red blood cells parasitized by Plasmodium falciparum, PNAS 105 (2008) 13730–13735.

[79] E.A. Evans, P.L. La Cell, Intrinsic material properties of the erythrocyte membrane indicated by mechanical analysis of deformation, Blood 45 (1975) 29–43.
[80] M. Puig-de-Morales-Marinkovic, K.T. Turner, J.P. Butler, J.J. Fredberg, S. Suresh, Viscoelasticity of the human red blood cell, Am. J. Physiol. Cell. Physiol. 293 (2007) C597–C605.
[81] Y.-Z. Yoon, J. Kotar, G. Yoon, P. Cicuta, The nonlinear mechanical response of the red blood cell, Phys. Biol. 5 (2008) 036007.
[82] S. Forconi, M. Guerrini, Do hemorheological laboratory assays have any clinical relevance? Clin. Hemorheol. 16 (1996) 17–22.
[83] D. Koutsouris, R. Guillet, J.C. Lelievre, M. Boynard, M.T. Guillemin, P. Bertholom, R.B. Wenby, Y. Beuzard, H.J. Meiselman, Individual red blood cell transit times during flow through cylindrical micropores, Clin. Hemorheol. 8 (1988) 453–459.
[84] O.K. Baskurt, Deformability of red blood cells from different species studied by resistive pulse shape analysis technique, Biorheology 33 (1996) 169–179.
[85] M.R. Clark, N. Mohandas, S.B. Shohet, Osmotic gradient ektacytometry: Comprehensive characterization of red cell volume and surface maintenance, Blood 61 (1983) 899–910.
[86] H. Schmid-Schönbein, P. Gaehtgens, T. Fischer, M. Stöhr-Liesen, Biology of red cells: Non-nucleated erythrocytes as fluid drop-like cell fragments, Int. J. Microcirc. Clin. Exp. 3 (1984) 161–196.
[87] J.G.G. Dobbe, G.J. Streekstra, M.R. Hardeman, C. Ince, C.A. Grimbergen, Measurement of the distribution of red blood cell deformability using an automated rheoscope, Cytometry 50 (2002) 313–325.
[88] M. Mason Guest, T.P. Bond, R.G. Cooper, J.R. Derrick, Red blood cells: Change in shape in capillaries, Science 142 (1963) 1319–1321.
[89] J. Seki, H.H. Lipowsky, In vivo and in vitro measurements of red cell velocity under epifluorescence microscopy, Microvasc. Res. 38 (1989) 110–124.
[90] J.H. Jeong, Y. Sugii, M. Minamiyama, K. Okamoto, Measurement of RBC deformation and velocity in capillaries in vivo, Microvasc. Res. 71 (2006) 212–217.
[91] G.J. Tangelder, D.W. Slaaf, A.M.M. Muijtjens, T. Arts, M.G.A. oude Egbrink, R.S. Reneman, Velocity profiles of blood platelets and red blood cells flowing in arterioles of the rabbit mesentery, Circ. Res. 59 (1986) 505–514.
[92] U. Bagge, P.I. Branemark, R. Karlsson, R. Skalak, Three-dimensional observations of red blood cell deformation in capillaries, Blood Cells 6 (1980) 231–239.
[93] R. Skalak, P.I. Branemark, Deformation of red blood cells in capillaries, Science 164 (1969) 717–719.
[94] P. Gaehtgens, C. Duhrssen, K.H. Albrecht, Motion, deformation, and interaction of blood cells and plasma during flow through narrow capillary tubes, Blood Cells 6 (1980) 799–812.
[95] G. Tomaiuolo, M. Simeone, V. Martinelli, B. Rotoli, S. Guido, Red blood cell deformability in microconfined shear flow, Soft Matter 5 (2009) 3736–3740.
[96] P. Gaehtgens, H. Schmid-Schönbein, Mechanisms of dynamic flow adaptation of mammalian erythrocytes, Naturwissenschaften 69 (1982) 294–296.
[97] R. Hsu, T.W. Secomb, Motion of nonaxisymmetric red blood cells in cylindrical capillaries, J. Biomech. Eng. 111 (1989) 147–151.
[98] T.W. Secomb, R. Skalak, N. Ozkaya, J.F. Gross, Flow of axisymmetric red blood cells in narrow capillaries, J. Fluid Mech. 163 (1986) 405–423.
[99] R.M. Hochmuth, R.N. Marple, S.P. Sutera, Capillary blood flow. I. Erythrocyte deformation in glass capillaries, Microvasc. Res. 2 (1970) 409–419.
[100] S. Reitsma, D.W. Slaaf, H. Vink, M.A. van Zandvoort, M.G. oude Egbrink, The endothelial glycocalyx: Composition, functions, and visualization, Pflügers Archiv: Eur. J. Physiol. 454 (2007) 345–359.
[101] A.R. Pries, T.W. Secomb, T. Gessner, M.B. Sperandio, J.F. Gross, P. Gaehtgens, Resistance to blood flow in microvessels in vivo, Circ. Res. 75 (1994) 904–915.
[102] K.H. Albrecht, P. Gaehtgens, A. Pries, M. Heuser, The Fahraeus effect in narrow capillaries (i.d. 3.3 to 11.0 μm), Microvasc. Res. 18 (1979) 33–47.
[103] A. Bransky, N. Korin, Y. Nemirovski, U. Dinnar, Correlation between erythrocytes deformability and size: A study using a microchannel based cell analyzer, Microvasc. Res. 73 (2007) 7–13.
[104] A.C.L. Barnard, L. Lopez, J.D. Hellums, Basic theory of blood flow in capillaries, Microvasc. Res. 1 (1986) 23–34.
[105] M.J. Lighthill, Pressure-forcing of tightly fitting pellets along fluid-filled elastic tubes, J. Fluid Mech. 34 (1968) 113–143.
[106] R. Bali, S. Mishra, S. Dubey, A mathematical model for red cell motion in narrow capillary surrounded by tissue, Appl. Math. Comp. 196 (2008) 193–199.
[107] T.W. Secomb, Flow-dependent rheological properties of blood in capillaries, Microvasc. Res. 34 (1987) 46–58.
[108] E.A. Evans, R. Skalak, Mechanics and Thermodynamics of Biomembranes, CRC, Boca Raton, FL, 1980.
[109] O.K. Baskurt, M. Boynard, G.C. Cokelet, P. Connes, B.M. Cooke, S. Forconi, F. Liao, M.R. Hardeman, F. Jung, H.J. Meiselman, G. Nash, N. Nemeth, B. Neu, B. Sandhagen, S. Shin, G. Thurston, J.L. Wautier, New guidelines for hemorheological laboratory techniques, Clin. Hemorheol. Microcircul. 42 (2009) 75–97.
[110] A. Palmer, A study of blood flow in minute vessels of the pancreatic region of the rat with reference to intermittent corpuscular flow in individual capillaries, Quart. J. Exp. Physiol. 44 (1959) 149.
[111] V. Seshadri, R.M. Hochmuth, P.A. Croce, S.P. Sutera, Capillary blood flow. III. Deformable model cells compared to erythrocytes in vitro, Microvasc. Res. 2 (1970) 434–442.
[112] P.R. Zarda, S. Chien, R. Skalak, Elastic deformations of red blood cells, Biorheology 10 (1978) 211–221.
[113] T.W. Secomb, R. Skalak, A two-dimensional model for capillary flow of an asymmetric cell, Microvasc. Res. 24 (1982) 194–203.
[114] T.W. Secomb, R. Hsu, A.R. Pries, A model for RBC motion in glycocalyx-lined capillaries, Am. J. Physiol. 274 (1998) H1016–H1022.
[115] E.R. Damiano, The effect of the endothelial-cell glycocalyx on the motion of red blood cells through capillaries, Microvasc. Res. 55 (1998) 77–91.

[116] T.W. Secomb, R. Hsu, Analysis of red blood cell motion through cylindrical micropores: Effects of cell properties, Biophys. J. 71 (1996) 1095–1101.
[117] C. Pozrikidis, Numerical simulation of the flow-induced deformation of red blood cells, Ann. Biomed. Eng. 31 (2003) 1194.
[118] C. Pozrikidis, Axisymmetric motion of a file of red blood cells through capillaries, Phys. Fluids 17 (2005) 031503.
[119] C. Pozrikidis, Numerical simulation of cell motion in tube flow, Ann. Biomed. Eng. 33 (2005) 165–178.
[120] S.K. Boey, D.H. Boal, D.E. Discher, Simulations of the erythrocyte cytoskeleton at large deformation. I. Microscopic models, Biophys. J. 75 (1998) 1573–1583.
[121] D.E. Discher, D.H. Boal, S.K. Boey, Simulations of the erythrocyte cytoskeleton at large deformation. II. Micropipette aspiration, Biophys. J. 75 (1998) 1584–1597.
[122] J. Li, G. Lykotrafitis, M. Dao, S. Suresh, Cytoskeletal dynamics of human erythrocyte, PNAS 104 (2007) 4937–4942.
[123] H. Noguchi, G. Gompper, Shape transitions of fluid vesicles and red blood cells in capillary flows, PNAS 102 (2005) 14159–14164.
[124] J.L. McWhirter, H. Noguchi, G. Gompper, Flow-induced clustering and alignment of vesicles and red blood cells in microcapillaries, PNAS 106 (2009) 6039–6043.
[125] I.V. Pivkin, G.E. Karniadakis, Accurate coarse-grained modeling of red blood cells, Phys. Rev. Lett. 101 (2008) 118105.
[126] Y. Kikuchi, K. Sato, H. Ohki, T. Kaneko, Optically accessible microchannels formed in a single-crystal silicon substrate for studies of blood rheology, Microvasc. Res. 44 (1992) 226–240.
[127] Y. Kikuchi, Q. Da, T. Fujino, Variation in red blood cell deformability and possible consequences for oxygen transport to tissue, Microvasc. Res. 47 (1994) 222–231.
[128] P. Wilding, J. Pfahler, H.H. Bau, J.N. Zemel, L.J. Kricka, Manipulation and flow of biological fluids in straight channels micromachined in silicon, Clin. Chem. 40 (1994) 43–47.
[129] G.R. Cokelet, R. Soave, G. Pugh, L. Rathbun, Fabrication of in vitro microvascular blood flow systems by photolithography, Microvasc. Res. 46 (1993) 394–400.
[130] M.C. Tracey, R.S. Greenaway, A. Das, P.H. Kaye, A.J. Barnes, A silicon micromachined device for use in blood cell deformability studies, IEEE Trans. Biomed. Eng. 42 (1995) 751–761.
[131] N. Sutton, M.C. Tracey, I.D. Johnston, R.S. Greenaway, M.W. Rampling, A novel instrument for studying the flow behaviour of erythrocytes through microchannels simulating human blood capillaries, Microvasc. Res. 53 (1997) 272–281.
[132] J.P. Brody, Y. Han, R.H. Austin, M. Bitensky, Deformation and flow of red blood cells in a synthetic lattice: Evidence for an active cytoskeleton, Biophys. J. 68 (1995) 2224–2232.
[133] K. Tsukada, E. Sekizuka, C. Oshio, H. Minamitani, Direct measurement of erythrocyte deformability in diabetes mellitus with a transparent microchannel capillary model and high-speed video camera system, Microvasc. Res. 61 (2001) 231–239.
[134] J.P. Shelby, J. White, K. Ganesan, P.K. Rathod, D.T. Chiu, A microfluidic model for single-cell capillary obstruction by Plasmodium falciparum infected erythrocytes, PNAS 100 (2003) 14618–14622.
[135] M. Abkarian, M. Faivre, H.A. Stone, High-speed microfluidic differential manometer for cellular-scale hydrodynamics, PNAS 103 (2006) 538–542.
[136] R. Zhao, J.F. Antaki, T. Naik, T.N. Bachman, M.V. Kameneva, Z.J. Wu, Microscopic investigation of erythrocyte deformation dynamics, Biorheology 43 (2006) 747–765.
[137] G. Danker, P.M. Vlahovska, C. Misbah, Vesicles in Poiseuille flow, Phys. Rev. Lett. 102 (2009) 148102.
[138] M. Faivre, M. Abkarian, K. Bickraj, H.A. Stone, Geometrical focusing of cells in a microfluidic device: An approach to separate blood plasma, Biorheology 43 (2006) 147–159.
[139] S.S. Shevkoplyas, S.C. Gifford, T. Yoshida, M.W. Bitensky, Prototype of an in vitro model of the microcirculation, Microvasc. Res. 65 (2003) 132–136.
[140] S.S. Shevkoplyas, T. Yoshida, S.C. Gifford, M.W. Bitensky, Direct measurement of the impact of impaired erythrocyte deformability on microvascular network perfusion in a microfluidic device, Lab Chip 6 (2006) 914–920.
[141] S. Suresh, Mechanical response of human red blood cells in health and disease: Some structure–property–function relationships, J. Mater. Res. 21 (2006) 1871–1877.
[142] A.C. De Luca, G. Rusciano, R. Ciancia, V. Martinelli, G. Pesce, B. Rotoli, A. Sasso, Spectroscopical and mechanical characterization of normal and thalassemic red blood cells by Raman Tweezers, Opt. Express 16 (2008) 7943–7957.
[143] G. Barshtein, R. Ben-Ami, S. Yedgar, Role of red blood cell flow behavior in hemodynamics and hemostasis, Expert Rev. Cardiovasc. Ther. 5 (2007) 744–752.
[144] C. Quégunier, D. Barthés-Biesel, Axisymmetric motion of capsules through cylindrical channels, J. Fluid Mech. 348 (1997) 349–376.
[145] S.P. Sutera, V. Seshadri, P.A. Croce, R.M. Hochmuth, Capillary blood flow. II. Deformable model cells in tube flow, Microvasc. Res. 2 (1970) 420–433.
[146] V. Vitkova, M. Mader, T. Podgorski, Deformation of vesicles flowing through capillaries, Europhys. Lett. 68 (2004) 398–404.
[147] F. Risso, F. Collé-Paillot, M. Zagzoule, Experimental investigation of a bioartificial capsule flowing in a narrow tube, J. Fluid Mech. 547 (2006) 149–173.
[148] J.S. Lee, Y.C. Fung, Modeling experiments of a single red blood cell moving in a capillary blood vessel, Microvasc. Res. 1 (1969) 221–243.
[149] A. Diaz, N. Pelekasis, D. Barthès-Biesel, Transient response of a capsule subjected to varying flow conditions: Effect of internal fluid viscosity and membrane elasticity, Phys. Fluid 12 (2000) 948–957.
[150] H. Noguchi, G. Gompper, Vesicle dynamics in shear and capillary flows, J. Phys.: Condens. Matter 17 (2005) S3439–S3444.
[151] V. Sibillo, G. Pasquariello, M. Simeone, V. Cristini, S. Guido, Drop deformation in microconfined shear flow, Phys. Rev. Lett. 97 (2006) 054502.